TECHNICAL TRANSACTIONS 9/2017
CZASOPISMO TECHNICZNE 9/2017
MECHANICS
DOI: 10.4467/2353737XCT.17.161.7173

Filip Lisowski (filip.lisowski@mech.pk.edu.pl)
Faculty of Mechanical Engineering, Cracow University of Technology

Optimization of thread root undercut in the planetary roller screw

Optymalizacja podcięcia karbu gwintu w planetarnej przekładni śrubowej rolkowej

Abstract

The paper presents the optimization problem of a thread root undercut in the roller of planetary roller screw using FEM. The depth and shape of the undercut as well as the radii of thread profiles curvature were optimized for the series of cooperating threads. The maximum HMH reduced stress in the undercut was accepted as an objective function. The limitation to the maximum contact pressure was assumed. The procedure aimed at limiting the range of variables was accepted in order to improve the efficiency of optimization method.

Keywords: planetary roller screw, optimization, thread root undercut

Streszczenie

W artykule przedstawiono zagadnienie optymalizacji podcięcia dna karbu gwintu rolki w planetarnej przekładni śrubowej rolkowej z zastosowaniem MES. Optymalizowano głębokość i kształt podcięcia oraz promienie zaokrąglenia zarysu gwintów dla szeregu współpracujących zwojów śruby i rolki. Jako funkcję celu przyjęto maksymalne naprężenie w karbie gwintu rolki przy ograniczeniu na maksymalne naciski kontaktowe na powierzchniach współpracujących gwintów. W celu poprawy efektywności metody optymalizacji przyjęto procedurę, która ma na celu zawężenie przestrzeni zmiennych.

Słowa kluczowe: przekładnia śrubowa rolkowa, optymalizacja, podcięcie karbu gwintu

Denotations

d_s, d_r – pitch diameters of the screw and the roller [mm]
x_{s1}, x_{s2} – dimensions of straight thread root undercut [mm]
x_{e1}, x_{e2}, x_{e3} – dimensions of elliptical thread root undercut [mm]
x_{t1}, x_{t2}, x_{t3} – dimensions of triangular thread root undercut [mm]
R_s, R_r – radii of the screw and the roller thread flank [mm]
σ_{HMH}^{max} – maximum Huber-Mises-Hencky reduced stress in the thread root of the roller [MPa]
$\sigma_{HMH}^{max\_u}$ – maximum Huber-Mises-Hencky reduced stress in the undercut of the roller's thread root [MPa]
C_{press}^{max} – maximum contact pressure on thread (model without undercut) [MPa]
$C_{press}^{max\_u}$ – maximum contact pressure on thread (model with undercut) [MPa]

1. Introduction

Planetary Roller Screw (PRS) is a type of linear actuator used to convert linear motion to rotational motion or in the other way round. Thanks to high operating parameters, the mechanism is used to carry heavy loads in demanding mechanical engineering applications [4]. The axial load between the screw and the nut is transferred through several rollers uniformly distributed around the screw. To synchronize the operation of rollers, two planetary gear transmissions are applied. Since the planetary gears and the ring gears are integral parts of the rollers and the nut, the design of gears engagement has a direct impact on the cooperation of the screw, rollers and nut threads [7].

In recent years, authors of several publications have addressed problems related to load distribution, thread outline as well as dynamic or contact analysis. In the paper [9], a computational model was presented to determine the load distribution between cooperating elements accepting an arbitrary number of rollers. The model was intended for preliminary design. The analysis of displacements and load distribution based on the simplified model was presented in [8]. The authors of publication [1] developed a hybrid model, using one-dimensional finite elements and nonlinear spring elements, required for computation of load distribution and axial stiffness. The authors of publication [3] analysed dynamic effects and efficiency of PRS. In the paper [6], deformations of single cooperating pair of screw-roller and nut-roller threads were estimated. The authors of publication [10] modeled elasto-plastic contact problems in the PRS and studied the effect of the profile radius of the roller thread on contact characteristics. In article [11], a model to determine contact positions and clearances of mating thread surfaces was proposed.

The goal of this paper was to apply the finite element method in the optimization of a thread root undercut for a 2D problem. The undercut was accepted in the roller's thread. Three shapes of the undercut (straight, elliptical and triangular) and their impact on the maximum reduced stress in the notch and contact pressure were considered.

2. Optimization problem

In order to solve an optimization problem, a 2D finite element model including 10 cooperating threads, the screw and the roller was accepted as shown in Fig. 1. The model consisted of around 24 000 nodes and 70 000 elements (depending on geometry of the undercut). The pitch diameters of the screw and the roller as well as the thread pitch were assumed as: d_s = 30 mm, d_r = 10 mm, p = 3 mm. The 8-node PLANE82 elements available in ANSYS software were used. The plane strain was accepted. The contact elements CONTA172 and TARGET169 were accepted. The coefficient of friction in the plane of the model was set to $\mu = 0.1$. The axial load F = 500 N was applied to the edge of the roller core. Young modulus $E = 2.11 \cdot 10^5$ MPa and Poisson ratio $\nu = 0.3$ were accepted.

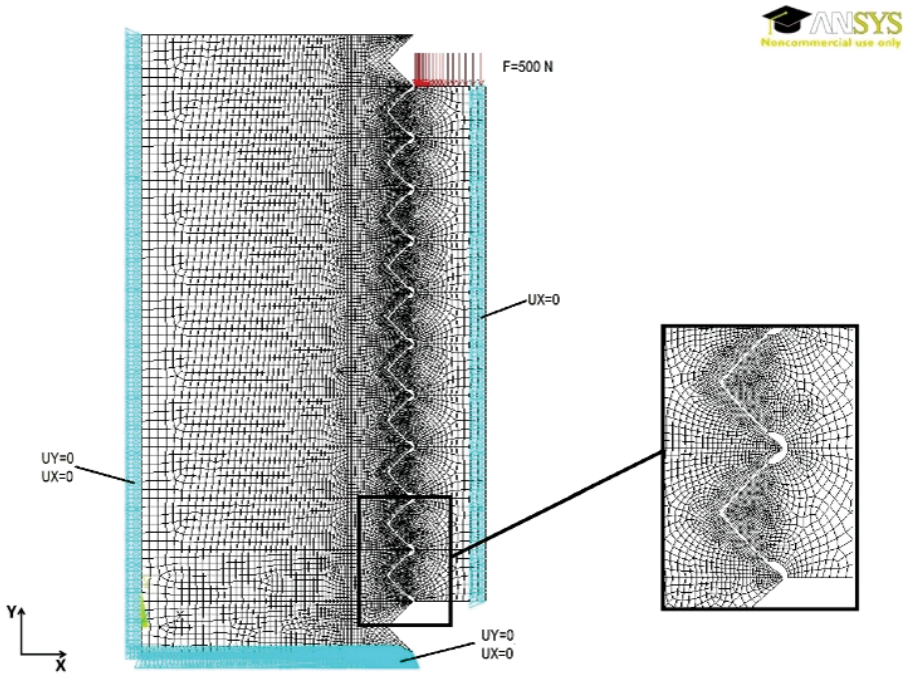

Fig. 1. Finite element model of the screw and the roller threads with boundary conditions

2.1. Optimization procedure

In order to improve the efficiency of optimization method, the procedure aimed at limiting the range of variables was accepted. To determine the starting points, a series of hundred calculations was performed. The values of design variables were randomly generated from the assumed range. The geometries resulted in the lowest HMH reduced stress were accepted as starting points. Optimization problem was solved by applying the gradient method available in ANSYS.

2.2. Objective function

As an objective function, Huber-Mises-Hencky reduced stress in the thread root undercut was accepted. The aim of the optimization was to determine the minimum of the function given by Eq. 1.

$$Q(x_{ij}, Rr, k) = \sigma_{HMH}^{max\_u} \tag{1}$$

$$Q \rightarrow \min \tag{2}$$

where:

Q – objective function,
$\sigma_{HMH}^{max\_u}$ – Huber-Mises-Hencky reduced stress in the thread undercut,
x_{ij}, R_r, k – design variables.

2.3. Design and state variables

The authors of paper [2] noticed that, in order to keep the constant rolling diameters of cooperating elements, the thread profile of at least one of them has to be curved. The most advantageous distribution of the contact pressure is obtained when one of the thread profile is convex, whereas the other one is concave [5]. In this paper, the profile of the roller thread was assumed to be convex whereas the profile of the screw to be concave. The geometries of straight, elliptical and triangular thread root undercut are presented in Figs. 2–4. The values of design variables accepted for starting points as well as resulted maximum HMH reduced stress and maximum contact pressure for these points are presented in Tables 1–3.

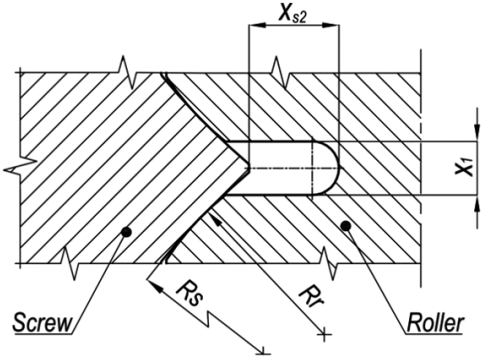

Fig. 2. Design variables and dimensions of threads with straight undercut

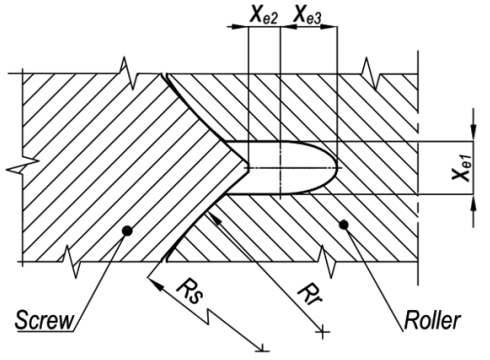

Fig. 3. Design variables and dimensions of threads with elliptical undercut

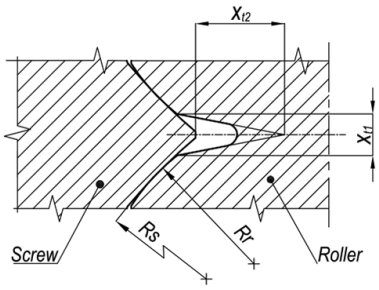

Fig. 4. Design variables and dimensions of threads with triangular undercut

Table 1. Design and state variables and optimization starting points
(straight undercut of roller's thread root)

Design variables	***Sp*1**	***Sp*2**	***Sp*3**	***Sp*4**	**Restrictions**
x_{s1}	0.75	0.88	0.81	0.96	$0.1 < x_{s1} < 1$
x_{s2}	0.10	0.10	0.10	0.10	$0.1 < x_{s2} < 1$
R_r	8.16	14.48	15.14	15.86	$2 < R_r < 20$
k	1.64	1.26	1.23	1.60	$1.1 < R_r < 2$
State variables					
R_S	13.38	18.58	18.62	25.38	–
$c_{press}^{max\_u}$	370	243	216	282	$C_{press}^{max\_u} < 0.6\, C_{press}^{max}$
Obj. function					
$\sigma_{HMH}^{max\_u}$	183	169	174	166	–

Table 2. Design and state variables and optimization starting points
(elliptical undercut of roller's thread root)

Design variables	***Sp*1**	***Sp*2**	***Sp*3**	***Sp*4**	Restrictions
x_{e2}	0.76	0.88	0.81	0.84	$-1 < x_{e2} < -0.1$
x_{e3}	1.40	1.30	1.02	1.04	$0.1 < x_{e3} < 1$
R_r	16.70	19.25	18.14	11.93	$2 < R_r < 20$
k	1.27	1.74	2.00	1.42	$1.1 < R_r < 2$
State variables					
x_{e1}	1.00	1.00	1.00	1.00	
R_S	21.21	33.50	36.28	16.94	–
$c_{press}^{max\_u}$	312	297	324	311	$C_{press}^{max\_u} < 0.6\, C_{press}^{max}$
Obj. function					
$\sigma_{HMH}^{max\_u}$	206	216	222	223	–

Table 3. Design and state variables and optimization starting points
(triangular undercut of roller's thread root)

Design variables	*Sp*1	*Sp*2	*Sp*3	*Sp*4	Restrictions
x_{t2}	1.00	1.02	1.06	1.01	$0.1 < x_{t1} < -1$
x_{t3}	0.45	0.36	0.36	0.37	$0.25 < x_{t2} < 0.45$
R_r	20.00	10.21	16.57	9.37	$2 < R_r < 20$
k	1.10	1.56	1.68	1.48	$1.1 < R_r < 2$
State variables					
x_{t1}	1.00	1.00	1.00	1.00	–
R_S	22.00	15.93	27.84	13.87	
$c_{press}^{max\_u}$	191	326	282	281	$C_{press}^{max\_u} < 0.6\, C_{press}^{max}$
Obj. function					
$\sigma_{HMH}^{max\_u}$	160	220	199	193	–

2.4. Results

The dimensions of the optimal thread root undercut and resulted maximum HMH reduced stress in the thread root undercut as well as maximum contact pressure for the best results obtained for particular starting points are listed in tables 4–6. The results obtained for the geometry without undercut ($\sigma_{HMH}^{max\_u}$ = 308 MPa, C_{press}^{max} =184 MPa) were accepted as a reference point. The decrease of the maximum HMH reduced stress in the roller's thread undercut and the decrease of the maximum contact pressure for all of the considered shapes of thread root undercut are compared in Fig. 5. For the best result of the optimization problem, obtained for the triangular shape of undercut, the decrease of the maximum HMH reduced stress was 50% with an increase of the maximum contact pressure of 27%. It should be also noticed that the second best result was obtained for the straight undercut, where the decrease of the maximum HMH reduced stress equalled 48% and the decrease of the maximum contact pressure equalled 4%.

The distribution of HMH reduced stress obtained for the best result of optimization is shown in Fig. 6. Figs. 7–8 present the distribution of maximum HMH reduced stress in the thread root undercut and maximum contact pressure for all of the cooperating threads. Threads numeration starts from the top of model, where the load was applied.

Table 4. Design and state variables for the best optimization results
(straight undercut of the roller's thread root)

Design variables	*Sp*1	*Sp*2	*Sp*3	*Sp*4
x_{s1}	1.00	1.00	1.00	1.00
x_{s2}	0.10	0.10	0.10	0.40
R_r	17.04	15.51	15.77	10.86
k	1.19	1.20	1.12	1.15
State variables				
R_S	20.28	18.61	17.66	12.49
$c_{press}^{max\_u}$	181	206	176	238
$\sigma_{HMH}^{max\_u}$	179	162	160	266

Table 5. Design and state variables for the best optimization results (elliptical undercut of the roller's thread root)

Design variables	*Sp*1	*Sp*2	*Sp*3	*Sp*4
x_{e2}	–0.85	–0.40	–0.90	–0.90
x_{e3}	1.40	1.00	1.00	1.00
R_r	16.62	16.68	9.96	7.96
k	1.27	1.15	1.10	1.10
State variables				
x_{e1}	1.00	1.00	1.00	1.00
R_S	21.11	19.18	10.96	8.76
$c_{press}^{max\_u}$	251	238	206	226
$\sigma_{HMH}^{max\_u}$	305	266	196	201

Table 6. Design and state variables for the best optimization results (triangular undercut of the roller's thread root)

Design variables	*Sp*1	*Sp*2	*Sp*3	*Sp*4
x_{t2}	1.05	1.05	2.00	1.00
x_{t3}	0.45	0.45	0.45	0.45
R_r	15.93	7.05	16.55	6.05
k	1.21	1.19	1.23	1.10
State variables				
x_{t1}	1.00	1.00	1.00	1.00
R_S	24.05	8.39	20.36	6.66
$c_{press}^{max\_u}$	206	252	208	233
$\sigma_{HMH}^{max\_u}$	157	155	174	154

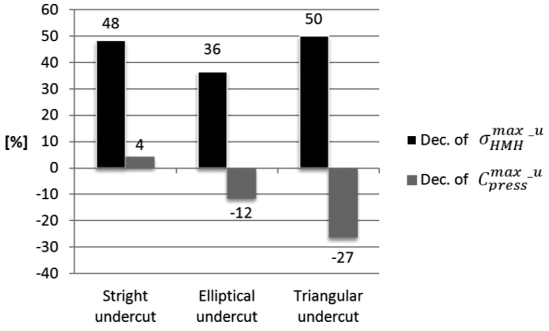

Fig. 5. Decrease of the maximum reduced stress in the thread root undercut and decrease of the maximum contact pressure on threads

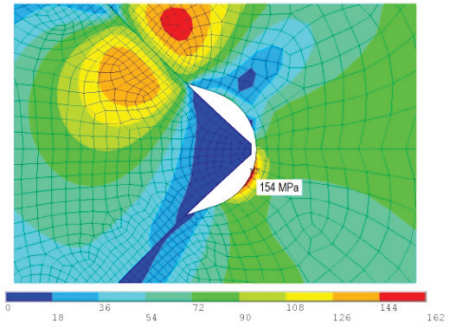

Fig. 6. Maximum HMH reduced stress in the triangular thread root undercut

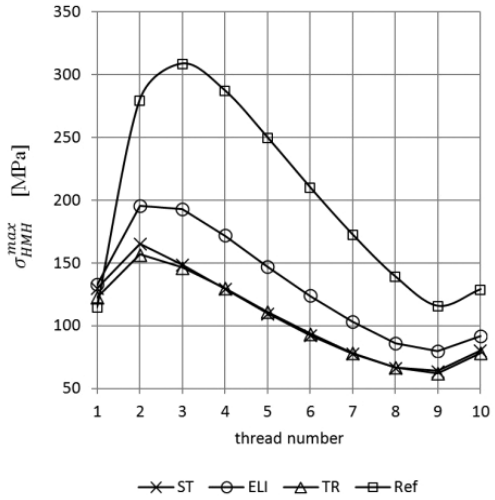

Fig. 7. Distribution of maximum HMH reduced stress in the roller's thread root

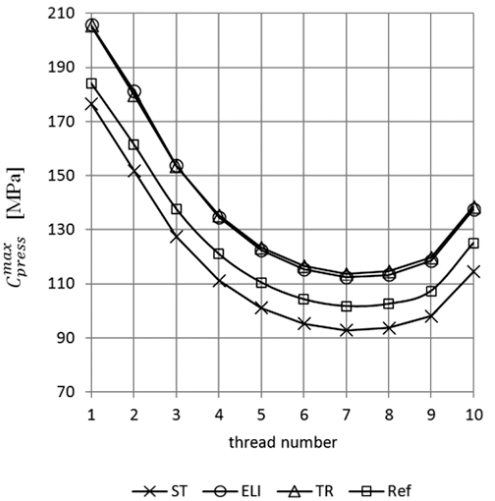

Fig. 8. Distribution of maximum contact pressure on threads

3. Conclusions

The results of the optimization problem, obtained by applying the finite element method indicated that the use of a thread root undercut in a roller is advantageous in the reduction of stress concentration in a thread notch. The best result was obtained for the triangular shape of an undercut. Concerning the cooperation of 10 pairs of the screw and roller threads, it can be concluded that dimensions of a triangular thread root undercut, referred to the thread pitch, should be accepted as follows: $x_{t1}/p \approx 0.33$, $x_{t2}/p \approx 0.35$, $x_{t3}/p \approx 0.15$.

Furthermore, it should be noted that the second best result was obtained for a straight undercut. In that case, the decrease of the maximum HMH reduced stress was slightly worse but the maximum contact pressure decreased by about 4%. Dimensions of straight thread root undercut should be accepted as follows: $x_{s1}/p \approx 0.33$, $x_{s2}/p \approx 0.03$.

References

[1] Abevi F., Daidie A., Chaussumier M., Sartor M., *Static load distribution and axial stiffness in a planetary screw mechanism*, Journal of Mechanical Design, 2015, Vol. 138, doi: 10.1115/1.4031859.

[2] Hojjat Y., Mahdi A.M., *A comprehensive study on capabilities and limitations of rollers crew with emphasis on slip tendency*, Mechanism and Machine Theory, Vol. 44, No. 10, 2009, 1887–1899.

[3] Jones M.H., Velinsky S.A., *Dynamics and Efficiency of the Planetary Roller Screw Mechanism*, Journal of Mechanisms and Robotics, 8(1), 2014, DOI:10.1115/1.4030082.

[4] Lisowski F., *Analiza obciążeń oraz optymalizacja konstrukcji wybranych śrubowych przekładni planetarnych*, Wydawnictwo Politechniki Krakowskiej, Kraków 2015, ISBN 978-83-7242-865-3, (in Polish).
[5] Lisowski F., *Optimization of a curvilinear thread profile in a planetary roller screw,* Technical Transactions, 2-M/2015, 149–156.
[6] Lisowski F., *Numerical computation of stresses and deformations in the planetary roller screw components*, Technical Transactions, 2-M/2015, 141–148.
[7] Lisowski F. Ryś J., *A methodology of designing the teeth conjugation in a planetary roller screw,* Archive of Mechanical Engineering, Vol. LXIII, No. 4, 2016, DOI: 10.1515/meceng-2016-0033.
[8] Lisowski F., *The Analysis of displacements and the load distribution between elements in a Planetary Roller Screw*, Applied Mechanics and Materials, 2014, 680, 361–364.
[9] Ryś J., Lisowski F., *The computational model of the load distribution between elements in a planetary roller screw*, Journal of Theoretical and Applied Mechanics, Vol. 52, No. 3, 2014.
[10] Tong R.T., Guo H., Liu G., Yao Q., *Elasto-plastic contact characteristics of the Planetary Roller Screw Mechanism*, Proceedings of the International Conference on Power Transmissions 2016 (ICPT 2016), Chongqing, P.R. China, 27–30 October 2016, 181– 186, DOI: 10.1201/9781315386829-28,
[11] Tong Fu X., Liu, G., Ma, S., Tong, R., Lim, T.C., *A comprehensive contact analysis of planetary roller screw mechanism*, Journal of Mechanical Design, Vol. 139, Issue 1, 2017, Article number 012302.